Mahajoni, V. V., and M. M. Sharma, "Mass Transfer in Packed Columns: Cocurrent (Downflow) Operation," *Chem. Eng. Sci.*, **35**, p. 941 (1980).
Rao, V. G., and A. A. H. Drinkenburg, "Pressure Drop and Hydrodynamic Properties of Pulses in Two-Phase Gas-Liquid Downflow through Packed Columns," *Can. Chem. Eng.*, **61**, p. 158 (1983).
Reiss, L. P., "Cocurrent Gas-Liquid Contacting in Packed Columns," *IEC Proc. Des. Dev.*, **6**, p. 486 (1967).
Roberts, D., and P. V. Danckwerts, "Kinetics of Carbondioxide Absorption in Alkaline Solutions: Transient Absorption Rates and Catalysis by Arsenite," *Chem. Eng. Sci.*, **17**, p. 961 (1962).
Satterfield, C. N., "Trickle Bed Reactors," *AIChE J.* **21**, p. 209 (1975).
Sharma, M. M., and P. V. Danckwerts, "Chemical Methods of Measuring Interfacial Area and Mass Transfer Coefficients in Flow-Fluid Systems," *British Chem. Eng.*, **15**, p. 522 (1970).
Shende, B. W., and M. M. Sharma, "Mass Transfer in Packed Columns: Cocurrent Operation," *Chem. Eng. Sci.*, **29**, p. 1763 (1974).
Sylvester, N. D., and P. Pitayagulsarn, "Mass Transfer for Two-Phase Cocurrent Downflow in a Packed Bed," *IEC Proc. Des. Dev.*, **14**, p. 421 (1975).
Ufford, R. C., and J. J. Perona, "Liquid Phase Mass Transfer with Cocurrent Flow through Packed Towers," *AIChE J.*, **19**, p. 1223 (1973).
Wen, C. Y., and W. S. O'Brien, "Mass Transfer in Packed Beds Operated Cocurrently," *J. Chem. Eng. Data*, **8**, p. 42 (1963).

Manuscript received July 30, 1982; revision received May 3, and accepted May 10, 1983.

Low-Density Polyethylene Vessel Reactors

Part I: Steady State and Dynamic Modelling

By the use of a perfectly mixed model and an imperfectly mixed one for low-density polyethylene vessel reactors, we show that increases in the initiator consumption with polymerization temperature are due to mixing limitations at the initiator feed. With all its parameters independently estimated, the imperfectly mixed model provides an excellent agreement with experimental data for several initiators, feed flow rates and polymerization pressures. In the temperature region of industrial interest for each type of initiator, the open-loop reactor dynamics drastically change from open-loop unstable, at low temperatures, to open-loop stable at high polymerization temperatures.

LUIGI MARINI and CHRISTOS GEORGAKIS

Department of Chemical Engineering
Massachusetts Institute of Technology
Cambridge, MA 02139

SCOPE

The free radical polymerization of ethylene at high pressure is a reaction of broad commercial and engineering interest. In industrial practice, this process is undertaken either in autoclaves or in tubular reactors. Many engineering problems are involved in the design and operation of the vessel reactor, caused by the high values of operating pressure and temperature and by the necessity of removing the heat of polymerization. An accurate choice of conditions is essential to the economic operation of the process. Therefore, it is of practical importance to develop a mathematical model which predicts the dependence of reactor performance on the operating conditions. Furthermore, the dynamic behavior of the reactor might deviate from the desired one, leading to reactor extinction or sometimes to an explosion. For this reason it is also important to study the dynamic characteristics of the reactor.

Earlier efforts in analyzing the steady-state behavior of this high-pressure polyethylene process have been directed either to the tubular reactor (Agrawal and Dae Han, 1975; Chen et al., 1976) or to the ideal case of perfectly stirred continuous tank reactor (Goldstein and Hwa, 1966). Recently (van der Molen et al., 1981), a large number of experimental results has been published. They provide a comprehensive picture about the influence of the most important parameters on reactor performance. In particular, they clearly demonstrate the large increases in initiator consumption that characterize this process at relatively high temperatures for each type of initiator. The same data also provide a basis for the discussion of the stability characteristics of the reactor that lead to reaction extinction.

In the present paper we introduce two transient reactor models, the second of which accurately predicts all steady state and dynamic characteristics of the reactor experimentally observed. The model parameters are independently estimated and the excellent match between model predictions and experimental data is obtained without any parameter fit.

The first model (model A) considers the reactor perfectly mixed. The second model (model B) accounts in detail about the mixing phenomena near the initiator feed point.

CONCLUSIONS AND SIGNIFICANCE

The perfectly mixed model (model A) is in agreement with the experimental data at the region of low polymerization temperatures, but fails to account for the increases in initiator consumption observed at high temperatures. This phenomenon is accounted very accurately by the imperfectly mixed model (model B). With all its parameters independently estimated, model B shows an excellent agreement with experimental data

L. Marini was on leave from the Donegani Research Institute, Montedison Co., Via Fauser, Novara, Italy during the 1981–82 academic year.
Correspondence concerning this paper should be addressed to C. Georgakis, Department of Chemical Engineering, Lehigh University, Bethlehem, PA. 18015.

for different types of initiators, flow rates and reactor pressures. The model is also in excellent agreement with data obtained with a different reactor (Yamamoto and Sugimoto, 1979). Because of the predictive nature of this model one can conclude that the increase in initiator consumption takes place in the temperature region in which the decomposition time of the initiator becomes the same order of magnitude with the mixing time in the reactor region close to the feed point.

The examination of reactor dynamics through model A indicates that the steady state is unstable throughout the temperature range of interest. Model B shows that imperfect mixing has a stabilizing effect on reactor dynamics. As imperfect mixing increases the initiator consumption it also drastically reduces the value of the largest reactor eigenvalue, changing it from positive (open-loop unstable) to negative (open-loop stable) within the temperature region of interest for a given initiator. This implies that the dynamic characteristics of the reactor, operating at a given temperature can be drastically different depending on the initiator used. The dependence of light-off temperature on initiator type is also predicted in qualitative agreement with the respective experimental data.

INTRODUCTION

Various processes for the polymerization of ethylene have been described in the literature (Roff and Allison, 1965; Smith, 1964; Albright, 1974). Commercially available polyethylene is manufactured either by a low-pressure process which yields a high-density product or by the high-pressure process which yields low-density product. The higher-pressure process is usually a bulk polymerization one. This technique requires a highly purified ethylene feed and the operating pressure ranges between 1,000 and 3,000 atm.

Two main commercial reactor designs have been developed: the tubular reactor and the stirred vessel reactor. The vessel reactor is generally an autoclave with a high aspect ratio, divided into two or more compartments in series by fixed or rotating discs. The reaction requires a very high power input per unit volume to maintain good mixing conditions in each compartment. Because of the thickness of the wall, the low surface area, and the high heat load, the reactor can be considered practically adiabatic. Polymerization temperatures range between 150 and 300°C depending on the quality of product desired. Temperatures above 300°C are avoided, because of possible ethylene decomposition. Fresh ethylene is fed to each synthesis compartment together with a radical source, such as an azocompound or an organic peroxide, that decomposes and generates free radicals which start the polymerization reaction.

Interest on the effect that operating conditions and initiator efficiency have on the high-pressure ethylene polymerization process has clearly grown in the recent years (van der Molen et al., 1981; Luft et al., 1978; Luft and Seidl, 1980). On the other hand, this is due to the fact that initiator costs are an important fraction of the variable costs. Consequently the dependence of the amount of initiator consumed per polymer produced on the process conditions is of strong economic importance. On the other hand, the polymerization temperature is controlled through changes in the initiator feed flow, which has direct influence on the dynamic and stability behavior of the reactor.

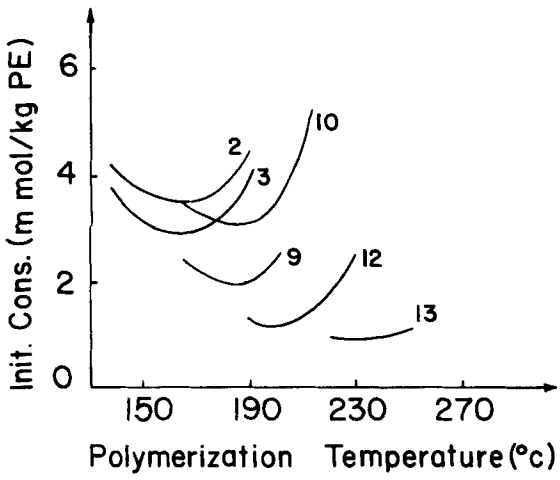

Figure 1. Specific initiator consumption as a function of polymerization temperature for various initiator types; experimental data from van der Molen and Koenen (1981).

It is known since 1970 (van der Molen and van Heerden, 1970) that the initiator productivity is not a simple function of reaction temperature and it is strongly influenced by other process conditions such as the degree of mixing in the reactor. However, it was only very recently (van der Molen and Koenen, 1981) that a sufficient number of experimental data relating initiator consumption and process conditions were published. They clearly show (Figure 1) that, in a given reactor, the initiator consumption per unit polymer produced is not a monotonic function of the reaction temperature and that it shows a minimum depending on the initiator type. Additional data show its dependence on mixing, pressure and input flow rate. Another phenomenon of parallel interest is the light-off temperature, below which the polymerization reactor becomes extinct. The data by van der Molen (1981) clearly demonstrate that this temperature also depends on initiator type and process conditions.

In a recent paper (Donati et al., 1981), it was shown that the effect of mixing is extremely important on reactor performance. It was pointed out that: a) the degree of mixing inside the reactor can be characterized by a recirculating flow caused by the impeller; and b) an imperfectly mixed reactor requires a higher initiator consumption per polymer produced than a perfectly stirred one operating at the same conditions.

This paper shows that these phenomena can be accounted for by a simple "imperfectly mixed" reactor model (model B). In particular, this model will be shown to match van der Molen's data (1981) very accurately, without any parameter fitting. Stability analysis of the same model provides important information on the dynamic characteristics of the reactor. To fully elucidate the effect of partial mixing on the performance of the reactor, a simple model (model A) is developed. This model assumes that the vessel reactor is completely mixed.

PERFECTLY MIXED MODEL

The perfectly mixed CSTR model (Model A) neglects any concentration or temperature gradient inside the reactor (Figure 2a). This assumption can be justified by the very high power input per unit volume usually given to this reactor (20 ÷ 100 kW/m^3); however, it does not account for the experimentally observed "mixing problems" (van der Molen, 1981; Yamamoto and Sugimoto, 1979). The polymerization reaction has been shown (Ehrlich and Mortimer, 1970) to proceed by a radical mechanism which takes place in a homogeneous phase. When only monomer conversion and initiator consumption must be computed, three reaction steps need to be considered: initiation, propagation and termination. Since the conversion in the industrial reactor is less than 15%, we will assume that the physical properties of the reacting medium do not change from input to output. Then the following mass and enthalpy balances can be easily derived:

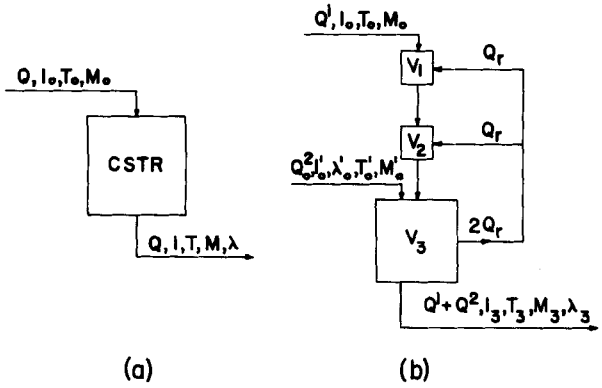

Figure 2. Schematic presentation of the two reactor models: (a) perfectly mixed model; (b) imperfectly mixed model.

$$V\frac{dI^*}{dt^*} = QI_o^* - QI^* - k_I I^* V \tag{1}$$

$$V\frac{d\lambda^*}{dt^*} = -Q\lambda^* + 2fk_I I^* V - k_T \lambda^{*2} V \tag{2}$$

$$V\frac{dM^*}{dt^*} = QM_o^* - QM^* - k_P \lambda^* M^* V \tag{3}$$

$$\rho C_P V\frac{dT^*}{dt^*} = \rho C_P Q(T_o^* - T^*) + (-\Delta H)k_P \lambda^* M^* V \tag{4}$$

We have here neglected the heat effect of the initiation and termination steps.

These equations can be made dimensionless by using as reference the known input steady-state values of the monomer and initiator compositions; the use of a reference temperature that is close to the temperature region, the reactor operates industrially.

$$\frac{dI}{dt} = I_o - I - Da_I I \exp(\gamma_I - \gamma_I/T) \tag{5}$$

$$\frac{d\lambda}{dt} = -\lambda + 2fDa_I I \exp(\gamma_I - \gamma_I/T) - Da_T \cdot \lambda^2 \exp(\gamma_T - \gamma_T/T) \tag{6}$$

$$\frac{dM}{dt} = 1 - M - Da_P \lambda M \exp(\gamma_P - \gamma_P/T) \tag{7}$$

$$\frac{dT}{dt} = T_o - T + \beta Da_P \lambda M \exp(\gamma_P - \gamma_P/T) \tag{8}$$

At steady state, the terms on the lefthand side are equal to zero, and a system of nonlinear algebraic equations is obtained. This can be easily solved by setting the reaction temperature T, and calculating the concentrations M, λ, I and the required initiator consumption I_o to sustain such a temperature:

$$M = 1 - (T - T_o)/\beta \tag{9}$$

$$\lambda = (T - T_o)/\beta Da_P M \exp(\gamma_P - \gamma_P/T) \tag{10}$$

$$I = \lambda(1 + Da_T \lambda \exp(\gamma_T - \gamma_T/T))/2fDa_I \exp(\gamma_I - \gamma_I/T) \tag{11}$$

$$I_o = I(1 + Da_I \exp(\gamma_I - \gamma_I/T)) \tag{12}$$

Two considerations must be clearly pointed out. First, it is well known (Ehrlich, 1970) that only the value of $k_P/\sqrt{k_T}$ can be derived from overall polymerization data. The individual values of the two parameters k_P and k_T are assumed to be equal to the ones used by Donati et al. (1981) and are in good agreement with the values used for other LDPE models (Chen et al., 1976; Agrawal and Dae Han, 1975). Particularly the termination rate, k_T, is assumed to be very fast and slightly dependent on temperature. On the other hand, the rate constants for the various initiators were derived from experimental tables presented by Akzo-Chemie, one of the most important initiator suppliers. They are in good agreement with other data (Luft, 1980) if the half life times of each initiator are compared in the temperature range commonly used. Table I summarizes the kinetic values for several initiators used in this paper.

TABLE I. REACTION RATE CONSTANTS: $K = K_o \exp(-(E + \Delta V(P - P_o))/RT)$

K_I for Initiator	K_o^* [L/s] [LT/mol·s]	E [cal/mol]	ΔV^a [cal/mol·atm]	f^b
2	$9.5\cdot10^{15}$	30,000.0	0.1	0.87
3	$1.3\cdot10^{16}$	30,120.0	0.1	0.96
9	$2.0\cdot10^{15}$	30,260.0	0.15	0.77
10	$5.8\cdot10^{15}$	31,200.0	0.15	0.60
12	$3.0\cdot10^{15}$	32,040.0	0.15	0.98
13	$3.4\cdot10^{15}$	34,500.0	0.15	0.95
21	$7.6\cdot10^{15}$	33,000.0	0.15	1.0
K_P	$1.25\cdot10^{8}$	7,420.0	−0.5	—
K_T	$5.0\cdot10^{9}$	1,000.0	0.0	—

[*] P_o is equal to 1 atm for K_I and equal to 1,301 atm for K_P.
[a] Estimated from van der Molen and Koenen (1981) and Luft et al. (1978).
[b] From van der Molen and Koenen (1981).

Curve I of Figure 3 shows the typical dependence of initiator consumption on polymerization temperature predicted by model A. It can be noted that, for a given initiator feed, the model predicts at least two possible steady-state temperatures. Calculations at temperatures much higher than those of industrial interest ($T >$ 300°C) show that model A can predict some additional steady states of limited practical use. One of the two steady state temperatures is very low ($T \doteq T_o$) and the other is in the region of industrial interest. In this region model A predicts a continuous decrease of initiator consumption with increasing reactor temperature. However, the experimental data of Figure 1 show that this is only true in the low-temperature part of the region of industrial interest. At the high-temperature part of this region (200–300°C), model A fails to accurately represent the experimentally observed dependence of the initiator consumption on reactor temperature.

Local stability analysis of the reactor can be obtained by linearizing Eqs. 5 to 8 of Model A around the steady state of interest and by computing the reactor eigenvalues by usual methods. The results of these calculations are shown in Curve I of Figure 4, where only the largest eigenvalue is plotted vs. reaction temperature. One

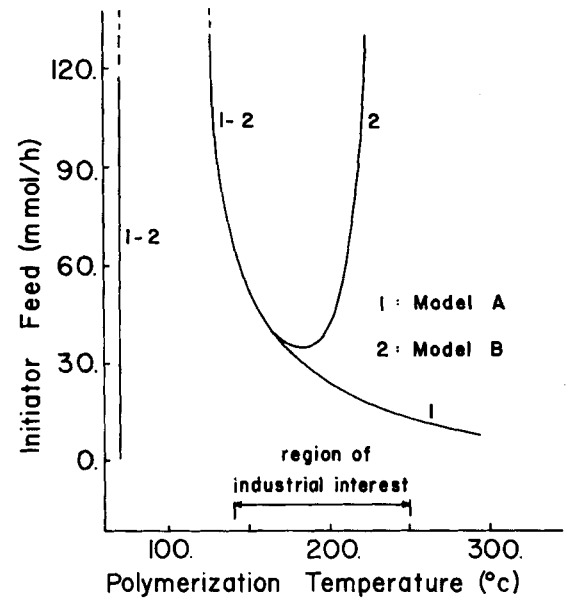

Figure 3. Model prediction of required initiator consumption as a function of polymerization temperature for model A (curve 1) and model B (curve 2). Q = 70 [kg/h]; $Q^1 = Q^2 = Q/2$; V = 1[LT]; $V_1 = V_2$ = 0.015 [LT]; Q_r = 250 [kg/h]; T_o = 70[°C]; P = 1,570 [atm]; initiator #10.

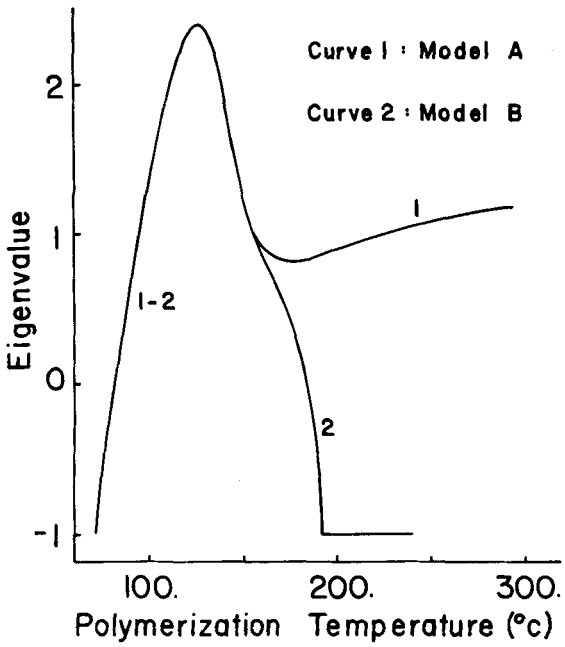

Figure 4. Model predictions for the dimensionless dominant eigenvalue dependence on polymerization temperature for model A (curve 1) and model B (curve 2). Model parameters as in Figure 3. Reference time constant τ = 26.9 [s].

clearly observes that the steady state in the region of industrial operation is characterized by a real positive eigenvalue. This implies that the reactor is predicted by model A to be open-loop unstable.

IMPERFECTLY MIXED MODEL

The failure of model A to present a qualitative agreement with the experimental data indicates that the assumption of perfect mixing might not be an accurate one at high temperatures, despite of the larger power input of LDPE vessel reactors. To further support this we pay close attention to the initiator balance, Eq. 5, from which we observe

$$I = \frac{I_o}{1 + Da_I \exp\left[\gamma_I\left(1 - \frac{1}{T}\right)\right]} \tag{13}$$

In the region where the initiator efficiency is experimentally found to decrease with temperature, the reaction term in the denominator becomes very high: $Da_I \exp[\gamma_I(1 - 1/T)] \gg 1$. This implies that the mean initiator concentration inside the reactor is much smaller than that at the feed. Consequently, the decomposition rate of the initiator is much higher near the feed point than in the bulk of the reactor. An increased amount of radicals is then produced near the feed point that are not effectively utilized throughout the reactor volume where most of the monomer is. With this observation in mind and by taking into account that the activation energy of the initiator decomposition reaction is much higher than that of propagation reaction (Table I), it seems reasonable to model the mixing characteristics near the feed point in more detail.

In Figure 2b, the entire vessel reactor is divided into three CSTR's in series. The first two CSTR's (V_1 and V_2), which account for a very small fraction of the total volume (3 ÷ 5%), are used to model the conditions at the initiator injection point, while the third CSTR (V_3) accounts for the remaining vessel volume where most of the polymerization reaction takes place. The action of the impeller in the compartment gives origin to a certain recirculating flow rate (Q_r) between the three volumes. As pointed out by Donati et al. (1981), the recirculating flow rate is generally much higher than the feed flow rate. Reasonable values for these fluid mechanical parameters of the imperfectly mixed model (model B) can be estimated from data by Donati et al. (1981) or can be computed by the jet theory model (Abramovich, 1963) as detailed in the Appendix.

Two different external feeds are used to model different operating conditions. The first one (Q_1) represents a cold feed of ethylene and initiator. The second one (Q_2) represents the flow of ethylene, radicals and polyethylene from another reaction zone in a multiple-zone reactor, or a pure ethylene flow at the top of the first zone used to cool the motor. In both cases, the second feed, Q_2, does not contain an appreciable amount of initiator, and it will be considered as entering the perfectly mixed zone (V_3).

The mathematical equations for this imperfectly mixed model consist of 12 differential equations, four for each of the three CSTR's. In their dimensionless form, they are written as follows:

$$\xi_1 \frac{dI_1}{dt} = \alpha I_0 + \epsilon I_3 - (\alpha + \epsilon) I_1 - \xi_1 Da_I I_1 \exp(\gamma_I - \gamma_I/T_1) \tag{14}$$

$$\xi_2 \frac{dI_2}{dt} = (\epsilon + \alpha) I_1 + \epsilon I_3 - (\alpha + 2\epsilon) I_2 - \xi_2 Da_I I_2 \exp(\gamma_I - \gamma_I/T_2) \tag{15}$$

$$\xi_3 \frac{dI_3}{dt} = (\alpha + 2\epsilon) I_2 + (1 - \alpha) I_0 - (1 + 2\epsilon) I_3 - \xi_3 Da_I I_3 \exp(\gamma_I - \gamma_I/T_3) \tag{16}$$

$$\xi_1 \frac{d\lambda_1}{dt} = \epsilon\lambda_3 - (\alpha + \epsilon)\lambda_1 + 2f\xi_1 Da_I I_1 \exp(\gamma_I - \gamma_I/T_1) + -\xi_1 Da_T \lambda_1^2 \exp(\gamma_T - \gamma_T/T_1) \tag{17}$$

$$\xi_2 \frac{d\lambda_2}{dt} = (\alpha + \epsilon)\lambda_1 + \epsilon\lambda_3 - (\alpha + 2\epsilon)\lambda_2 + 2f\xi_2 Da_I I_2 \exp(\gamma_I - \gamma_I/T_2) -\xi_2 Da_T \lambda_2^2 \exp(\gamma_T - \gamma_T/T_2) \tag{18}$$

$$\xi_3 \frac{d\lambda_3}{dt} = (\alpha + 2\epsilon)\lambda_2 + (1 - \alpha)\lambda_0' - (1 + 2\epsilon)\lambda_3 + 2f\xi_3 Da_I I_3 \exp(\gamma_I - \gamma_I/T_3) -\xi_3 Da_T \lambda_3^2 \exp(\gamma_T - \gamma_T/T_3) \tag{19}$$

$$\xi_1 \frac{dM_1}{dt} = \alpha + \epsilon M_3 - (\alpha + \epsilon) M_1 - \xi_1 Da_P M_1 \lambda_1 \exp(\gamma_P - \gamma_P/T_1) \tag{20}$$

$$\xi_2 \frac{dM_2}{dt} = (\alpha + \epsilon) M_1 + \epsilon M_3 - (\alpha + 2\epsilon) M_2 - \xi_2 Da_P M_2 \lambda_2 \exp(\gamma_P - \gamma_P/T_2) \tag{21}$$

$$\xi_3 \frac{dM_3}{dt} = (\alpha + 2\epsilon) M_2 + (1 - \alpha) M_0' - (1 + 2\epsilon) M_3 - \xi_3 Da_P M_3 \lambda_3 \exp(\gamma_P - \gamma_P/T_3) \tag{22}$$

$$\xi_1 \frac{dT_1}{dt} = \alpha T_0 + \epsilon T_3 - (\alpha + \epsilon) T_1 + \beta\xi_1 Da_P M_1 \lambda_1 \exp(\gamma_P - \gamma_P/T_1) \tag{23}$$

$$\xi_2 \frac{dT_2}{dt} = (\alpha + \epsilon) T_1 + \epsilon T_3 - (\alpha + 2\epsilon) T_2 + \beta\xi_2 Da_P M_2 \lambda_2 \exp(\gamma_P - \gamma_P/T_2) \tag{24}$$

$$\xi_3 \frac{dT_3}{dt} = (\alpha + 2\epsilon) T_2 + (1 - \alpha) T_0' - (1 + 2\epsilon) T_3 + \beta\xi_3 Da_P M_3 \lambda_3 \exp(\gamma_P - \gamma_P/T_3) \tag{25}$$

In the above equations the initiator and radical species concentrations ar made dimensionless with respect to a reference initiator concentration I_R^*. The dimensionless monomer concentration is defined with respect to the inlet monomer concentration and the dimensionless temperature with respect to a reference reactor

temperature which was taken as equal to 180°C for most of the calculations reported here. Furthermore, dimensionless time and the three *Da* numbers are defined with respect to the total residence time, τ, in the vessel reactor equal to $(V_1 + V_2 + V_3)/(Q_1 + Q_2)$. The second term in Eqs. 16, 19, 22 and 25 correspond to contribution of flow Q_2 in Figure 2b.

At steady state, the above model reduces to 12 nonlinear algebraic equations which are solved numerically to calculate the dependence of initiator consumption, I_o, on polymerization temperature. The local stability analysis can also be performed by linearization of Eqs. 14 to 25 and subsequent calculation of the eigenvalues for each steady state. One characteristic set of predictions for model B is given by curves II in Figures 3 and 4.

In Figure 3 we see that model B gives the same steady-state prediction with model A for low temperatures. At high temperatures model B predicts correctly the increase of the initiator consumption with temperature observed experimentally (van der Molen and Koenen, 1981). The difference between the predictions of models A (curve 1) and B (curve 2) in Figure 3 becomes quite apparent at 170°C. At this temperature one can estimate that the denominator in Eq. 13 becomes much higher than one. This implies that the decomposition time for the initiator has become quite smaller than the overall residence time in the reactor, necessitating the need of model B. Some order of magnitude calculation at 200°C for initiator #10 shows that its decomposition time is $\tau_I = 0.06$ s while the residence times in volumes V_1 and V_2 are $\tau_1 = 0.1$ and $\tau_2 = 0.05$ s, respectively, and the overall residence time in the reactor is $\tau = 27.0$ s. At the same temperature the polymerization time is of the order of 200 s. Even at higher temperatures, the polymerization time remains higher than the overall residence time indicating that the reactor can be considered perfectly mixed with respect to the propagation step. Model A becomes an inaccurate one at high temperatures, because the decomposition time for the initiator becomes quite smaller than τ necessitating the introductions of τ_1 and τ_2 through model B. Because of the increased decomposition rate for the initiator, the radicals produced are wasted in volumes V_1 and V_2 through the termination reaction without coming in good contact with the majority of the monomer that exists in volume V_3. This then clearly leads to the observed increases in initiator consumption with temperature.

The results of the stability analysis, Figure 4, show that model B predicts the reactor to become open-loop stable at high temperatures. Between 160 and 190°C the largest eigenvalue of model B drastically changes magnitude and from positive becomes quite negative. For temperatures higher than 200°C the dominant eigenvalue is independent of reactor temperature since it corresponds to the overall residence time of the reactor due to its adiabatic nature. The following remarks are of interest: 1. model B exhibits one additional possible steady temperature for a given initiator consumption than model A; and 2. imperfect mixing has a very desirable effect on the reactor dynamics (stabilization) when it adversely affects the steady-state characteristics (increased initiator consumption).

COMPARISON WITH EXPERIMENTAL DATA

To develop an understanding of the quantitative accuracy of model B we will now compare its predictions with the experimental data by van der Molen and Koenen (1981) for a LDPE reactor with a total volume of 1 L. These investigators tested many types of initiators under conditions representative of polymerization in commercial units, which corresponds to a residence time of 20 to 60 s and an operating pressure between 1,278 and 2,352 atm. They also used all the possible care to avoid clogging to the reactor wall due to phase separation, or any "hopper" problem due to the production of polymer of very high molecular weight. Part of the experimental results they reported is reproduced in Figure 1. In calculating its predictions none of the parameters for model B was adjusted. The kinetic parameters used were calculated independently, Table I, while the fluid mechanical parameters are calculated by the model given in the Appendix assuming (Figure A): $d_o = 5$ (mm), $L = 35$ (mm), $r = 12$ (mm), $n = 1500$ (rpm), $\beta = 8°$.

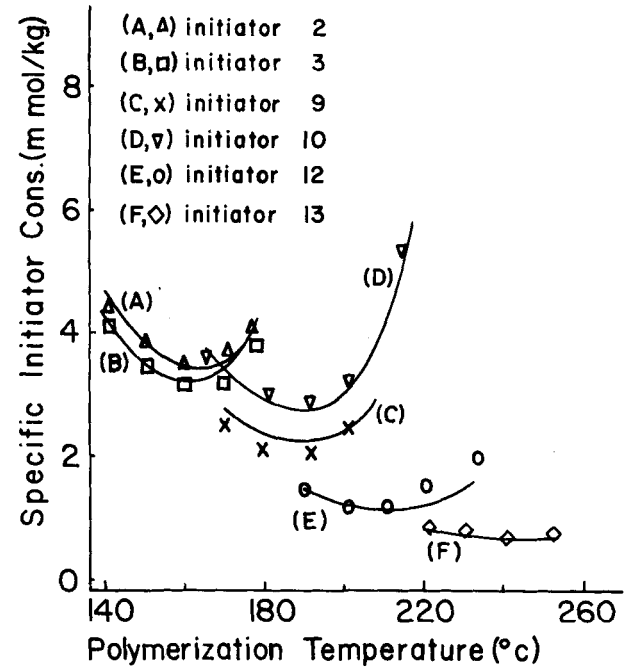

Figure 5. Comparison of model predictions with experimental data (van der Molen and Koenen, 1981) for the dependence of the specific initiator consumption on polymerization temperaturre for different initiator types. Pressure = 2,352 [atm]. Other model parameters as in Figure 3.

Comparisons of model B predictions with experimental data are presented in Figures 5–9. For the sake of conformity with the way the experimental data were presented, we have chosen to show the temperature dependence of the specific initiator consumption defined as the mol of initiator used per kg of polyethylene produced, which is proportional to $I_o/(1 - M_3)$. In Figure 5 comparisons between model predictions and experimental data show an excellent agreement for six different types of initiators and a wide range of polymerization temperatures.

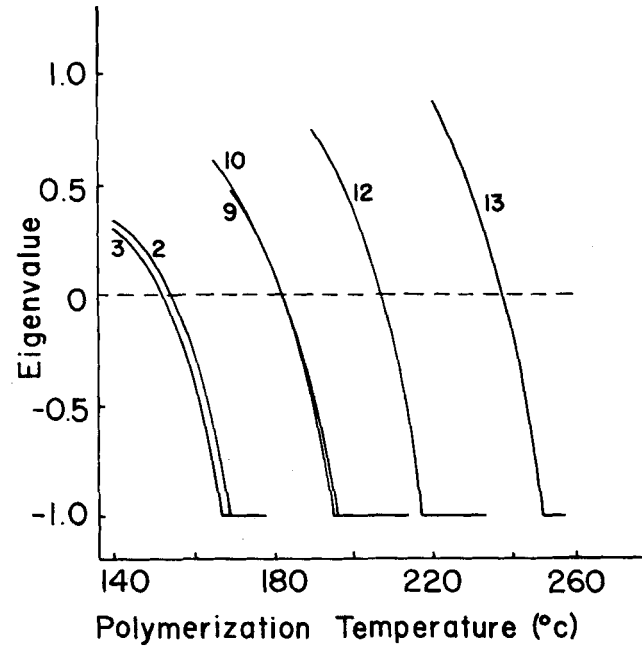

Figure 6. Model predictions for the dimensionless dominant eigenvalue dependence on polymerization temperature for various initiator types. Same conditions as in Figure 5. Reference time constant $\tau = 26.9$ [s].

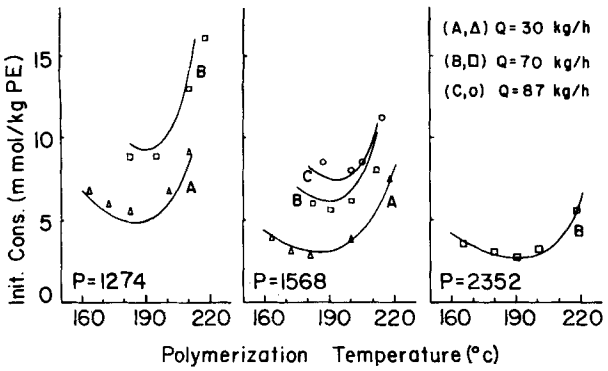

Figure 7. Comparison of model predictions with experimental data (van der Molen and Koenen, 1981) for the dependence of specific initiator consumption on polymerization temperature. Different flow rates (Q) and different polymerization pressures (P). Initiator #10. Other model parameters as in Figure 3.

The corresponding results of local stability analysis for the various initiators studied are reported in Figure 6. They shed light on the reasons why each initiator can be industrially used only in a very narrow temperature range. If we consider, for example, the 2-ethylhexyl-peroxidicarbonate initiator (initiator #3) it is known that it can be employed industrially in the temperature range between 140 and 170°C. Figure 6 shows that at temperatures lower than 140°C the open-loop reactor eigenvalue corresponding to this initiator becomes quite high and positive, which generates difficulties for the effective control of the reactor. On the other hand, at polymerization temperatures close to 170°C the reactor is open-loop stable, but the specific initiator consumption has increased making it desirable to use another initiator such as #9. This initiator change from #3 to #9 at the same polymerization temperature decreases the mmol of initiator need per kg of polymer produced. At the same time, it drastically changes the open-loop dynamics of the reactor from quite stable (initiator #3 at 170°C) to quite unstable (initiator #9 at 170°C) as it is clearly seen in Figure 6. Similar arguments can be used to explain why terbutyl-peroxi-2-ethylexanoate (initiator #13) is used industrially only when the polymerization temperature is higher than 220°C.

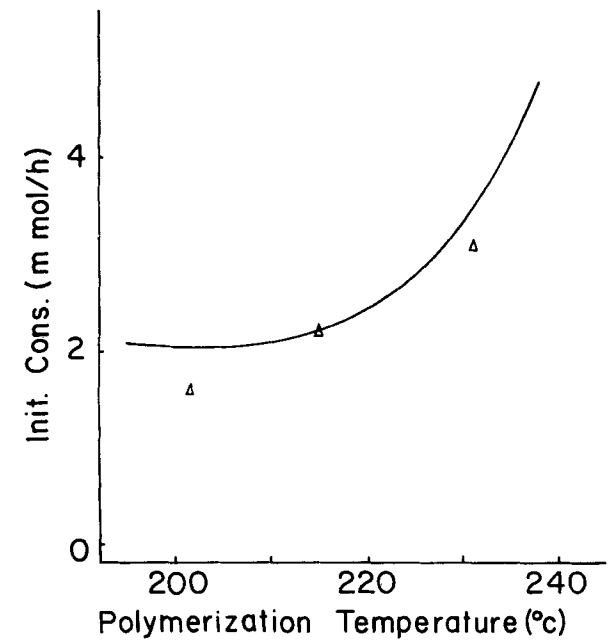

Figure 8. Comparison of model predictions with experimental data (Yamamoto and Sugimoto, 1979) for the dependence of initiator consumpton on polymerization temperature. Q = 43 [kg/h]; $Q^1 = Q^2 = Q/2$; V = 1.46 [LT]; $V_1 = V_2$ = 0.022 [LT]; Q_r = 250 [kg/h]; T_o = 70[°C]; P = 2,400 [atm]; initiator #21.

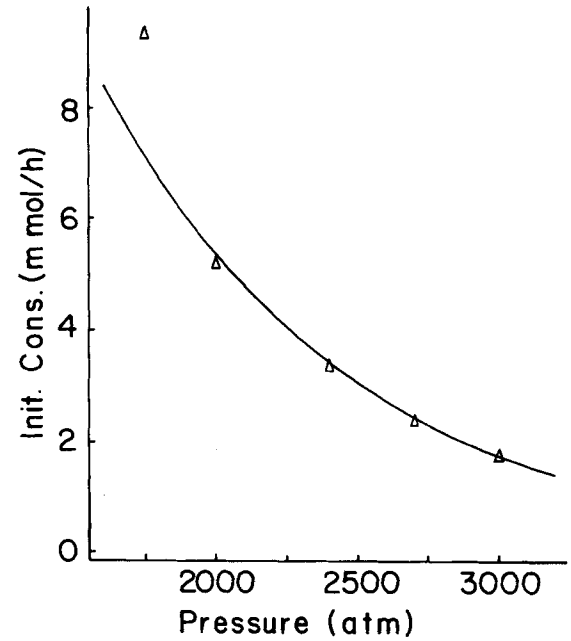

Figure 9. Comparison of model predictions with experimental data (Yamamoto and Sugimoto, 1979) for the dependence of initiator consumption on polymerization pressure. Temperature = 230[°C]. Other model parameters as in Fig. 8.

van der Molen and Koenen (1981) also reported "light-off temperature" for each type of initiator studied. Since their experimental reactor must have been under some closed-loop feed-back control, the light-off temperatures they reported is closely related to the temperatures at which the closed-loop eigenvalues become zero. Direct comparison with the corresponding model predictions is not possible since no information is available for the controller gains used in the experimental reactor. Instead of guessing the controller gains, we can calculate the light-off temperature from Figure 6 for the case of no feed-back action, that is, the temperature at which the open loop eigenvalue becomes zero. For initiator types #2, 3, 9, 10, 12 and 13 the corresponding "open-loop light-off temperatures" predicted by the model are 154, 152, 182, 182, 207 and 237°C, while the corresponding "closed-loop light-off temperatures" reported by van der Molen et al. (1981) are 130, 129, 156, 156, 178 and 210°C. We clearly do not expect the two sets of temperatures to be identical. The almost constant difference between the two sets is an indirect confirmation of the accuracy of the dynamic model.

Equally satisfactory agreement between model predictions and experimental data was also obtained for different flow rates and pressures (Figure 7). Local stability calculations showed that increased flow rates increase the open-loop eigenvalue which increases the light-off temperature. On the other hand, it was found that the model predicts a negligible effect of pressure on the light-off temperature. Both these trends are in agreement with the experimental data (van der Molen and Koenen, 1981). The mixing parameters of the model were not changed when the pressure was decreased to its lowest value (1,278 atm), even though it is well known that, in small reactors, the pressure may play an important role in the mixing through its influence on polymer quality and the viscosity of the reacting medium.

The model was also compared against the experimental results of Yamamoto and Sugimoto (1979) who worked with a continuous stirred tank reactor with a total volume of 1.46 LT and a very high aspect ratio (L/D = 5). Although their primary purpose was to study the polymer quality, they give sufficient experimental details for a meaningful comparison with our model predictions. Since the stirring speed was the same as in van der Molen's reactor (n = 1,500 rpm), we will retain here the same relative size of the three CSTR's and recirculating flow rate. Our computed results are compared with their data in Figures 8 and 9. Figure 8 shows the

dependence of initiator consumption on temperature, and the dependence on reactor pressure is shown in Figure 9. Again, an excellent agreement between model predictions and experimental data is observed without any changes in the model parameters to improve the agreement. The initiator employed for these runs is tert-butylperoxiisobutyrate (#21).

We would also like to compare our models A and B with the model of Mercx, van der Molen and de Steenwinskel (1972) which will be called model C. It simulates the reactor as a Plus-Flow-with-Recycle, is only a steady state model. Although it is not predictive, it shows a minimum in the specific consumption of the initiator with temperature. Because the recycle ratio used is very high ($r = 300$) this model can easily be mistaken as a prefectly mixed one. However, this is not true because: 1. the predictions of model C resemble those of model B rather than those of model A; 2. at high temperatures the half life of the initiator becomes smaller than the internal circulation time in model C; and 3. the predictions of model C drastically change when the recycle ratio r is taken as infinite ($r \rightarrow \infty$). At that point the predictions of model C resemble those of model A. Obviously, a recycle ratio equal to 300 is not sufficient for model C to be considered as a well-mixed model.

ACKNOWLEDGMENT

The authors are greatly indebted to the Donegani Research Institute, of the Montedison Co., Novara (Italy), for the approval and financial support of Marini's year-long visit at MIT. We are also grateful to the Camille and Henry Dreyfus Foundation for the award to Christos Georgakis of a Dreyfus Teacher-Scholar Grant which greatly contributed to this research. One of the reviewers is acknowledged for bringing the model of Mercx et al. to our attention.

NOTATION

Cp	= specific heat (0.57 kcal/kg·°C)
E_I, E_P, E_T	= activation energy (cal/mol)
f	= initiator efficiency factor
$(-\Delta H)$	= heat of polymerization (21.4 kcal/mol)
I^*	= initiator concentration (mol/LT)
k_I, k_P, k_T	= rate constants
M^*	= monomer concentration (mol/LT)
P	= pressure (atm)
Q	= flow rate (LT/s)
Q_r	= recirculating flow rate (LT/s)
t^*	= time (s)
T^*	= temperature (K)
V	= volume (LT)
ΔV	= activation volume (cal/mol·atm)
ρ	= density (0.524 kg/LT)
λ^*	= radicals concentration (mol/LT)
τ	= residence time (s)

Subscripts

0	= input conditions
1	= volume 1
2	= volume 2
3	= volume 3
I	= initiation
P	= propagation
T	= termination
R	= reference condition

Superscripts

1	= feed 1
2	= feed 2
*	= dimensional variable

Dimensionless Variables

$$\xi_i = \frac{V_i}{V} \quad (i = 1,2,3)$$

$$\epsilon = \frac{Q_r}{Q_1 + Q_2}$$

$$\alpha = \frac{Q_1}{Q_1 + Q_2}$$

$$I = I^*/I_R^* \qquad I_o = I_o^*/I_R^*$$
$$\lambda = \lambda^*/I_R^* \qquad M = M^*/M_O^*$$
$$T = T^*/T_R^* \qquad t = t^*/\tau$$
$$\gamma_I = E_I/RT_R^* \qquad \gamma_P = E_P/RT_R^* \qquad \gamma_T = E_T/RT_R^*$$
$$Da_I = k_I \exp(-\gamma_I)\tau$$
$$Da_P = k_p \exp(-\gamma_P)\tau I_R^*$$
$$Da_T = k_T \exp(-\gamma_T)\tau I_R^*$$

$$\beta = \frac{(-\Delta H)M_O^*}{\pi \cdot C_P \cdot T_R^*}$$

LITERATURE CITED

Abramovich, G. N., *The Theory of Turbulent Jets*, MIT Press, Cambridge, MA (1963).

Agrawal, S., and C. Dae Han, "Analysis of the High Pressure Polyethylene Tubular Reactor with Axial Mixing," *AIChE J.*, **21**, p. 449 (1975).

Albright, L. F., *Process for Major Addition Type Plastics and their Monomers*, McGraw Hill, New York (1974).

Chen C. H., J. G. Vermeychuk, J. A. Howell, and P. Ehrlich, "Computer Model for Tubular High Pressure Polyethylene Reactors," *AIChE J.*, **22**, 463 (1976).

Donati, G., M. Gramondo, E. Langianni, and L. Marini, "Low Density Polyethylene in Vessel Reactors," *Ing. Chim. Ital.*, **17**, p. 88 (1981).

Ehrlich, P., and G. A. Mortimer, "Fundamentals of Free Radical Polymerization of Ethylene," *Adv. in Polymer Sci.*, **7**, p. 386 (1970).

Goldstein, R., and C. S. Hwa, "Modelling and Analysis of Complex Reactors by Computer Simulation," ACS Symp. on Analysis of Complex Reaction System, Pittsburgh, PA (1966).

Luft, G., P. Herling, and H. Seidl, "Decomposition of Polymerization Initiators under High Pressure," *Die Angewandte Macromol.*, **73**, p. 95 (1978).

Luft, G., and H. Seidl, "Metering of Peroxide Polymerization Initiators at Elevated Pressure," *Die Angewandt Macromol.*, **86**, p. 93 (1980).

Mercx, F. J., Th.J van der Molen, and M. de Steenwinkel, "Relation Between Residence Time Distribution and Interior Productivity in the Continuous, High-Pressure Polymerization of Ethylene," 2nd Int. Symp. Chemical Reaction Engineering, Amsterdam (1972).

Raff, A. V., and J. B. Allison, *Polyethylene*, Interscience, New York (1956).

Smith, M. A., *Manufacture of Plastics*, Reinhold, New York (1964).

van der Molen, Th. J., and C. Van Heerden, "The effect of Imperfect Mixing on the Initiator Productivity in the High Pressure Radical Polymerization of Ethylene," *Adv. in Chemistry Ser.*, **109**, p. 92 (1970).

van der Molen, Th. J., and A. Koenen, "Effect of Process Conditions on 'light off' temperatures and consumption of 16 initiators, as determined from high pressure radical polymerization of ethylene," 7th Colloquium on Chem. Reac. Eng. Novara, Italy (1981).

Yamamoto, K., and M. Sugimoto, "Rate Constant for Long-Chain Branch Formation in Free-Radical Polymerization of Ethylene," *J. Macromol. Sci.-Chem.*, **A13** (8), p. 1067 (1979).

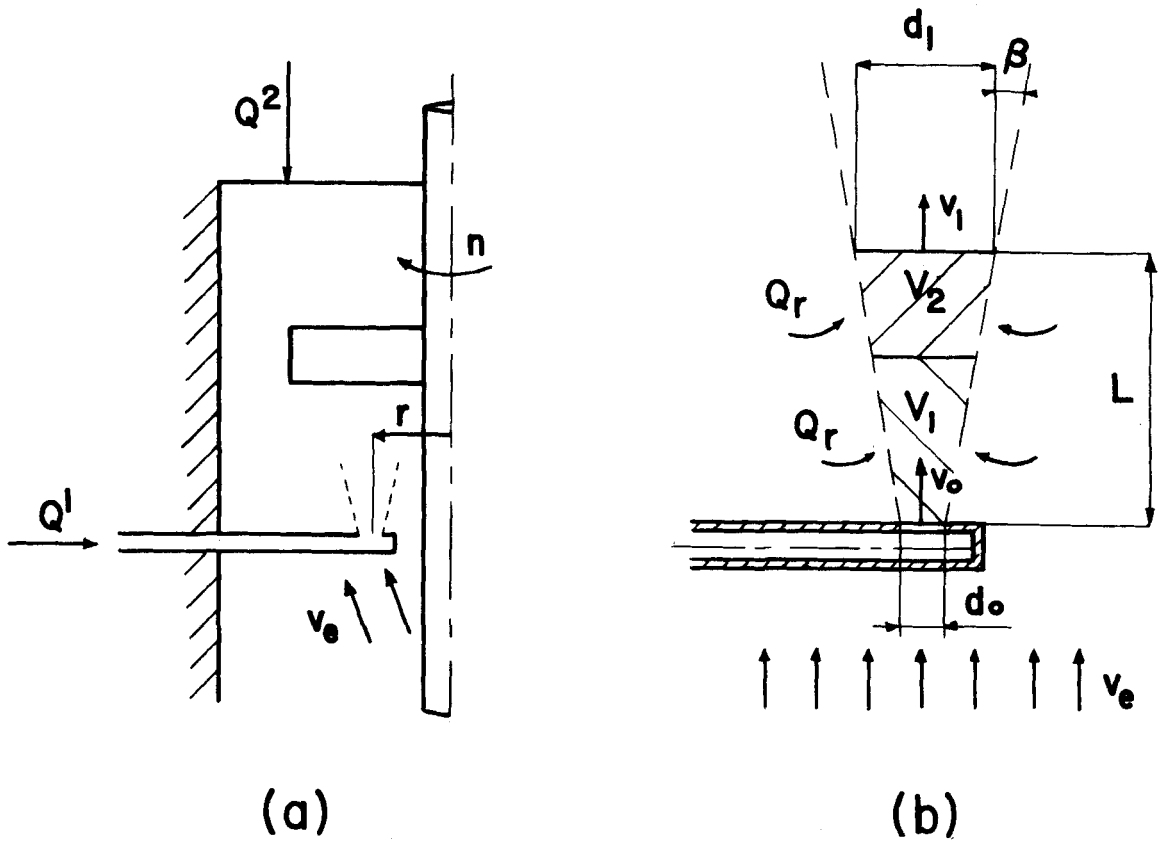

Figure A. Representation of the cold ethylene and initiator injection system into the reactor (a) and of its schematization for the calculation of model parameters (b).

APPENDIX: CALCULATION OF THE SIZE OF THE FIRST TWO VOLUMES (V_1 AND V_2) AND OF THE RECIRCULATING FLOW RATE (Q_r)

The injection of the initiator and cold ethylene feed into the vessel reactor is illustrated in Figure A. They are generally fed through a small pipe, not too close to the reactor wall, and not too far from the impeller. This gives origin to a small jet which spreads into the vessel and is continuously mixed with the surrounding fluid. Taking into account the very high level of power dissipation in the reactor, it seems reasonable to assume that the jet maintains a certain identity only in a small region near the injection point, after which it can be considered indistinguishable from the reacting medium. Moving away from the injection point, we find a continuous increase in the jet diameter, and a continuous entrainment of fluid into the jet region. With good approximation, we can model this situation with two volumes of equal size, each receiving one half of the total flow rate recirculated into the jet region.

To calculate the mixing parameters, we make the following two approximations: 1) the mixing between the input feed and the flow in the reactor is mainly due to the turbulence generated by the impeller. In fact, the input diameter (d_o in Figure A) cannot be too small, so that the output velocity of the jet is generally of the same order of magnitude, or less with the flow velocity inside the reactor; and 2) the jet spreads with a constant angle $\beta \cong 7 \div 10°$ (Abramowich, 1963). If the total length L of the jet region is fixed ($L/d_o \cong 4 \div 8$), we can calculate:

$$d_1 = d_o + 2Ltg\beta$$

$$V_T = \frac{\pi}{3} L \left(\frac{d_1^2}{4} + \frac{d_0^2}{4} + \frac{d_1 d_0}{4} \right)$$

$$V_1 = V_2 = V_T/2$$

The flow rate which enters into this volume and is mixed with the input flow rate depends essentially on the fluid velocity v_e, which can be estimated as:

$$v_e = \frac{2\pi rn}{60}$$

where n is the impeller rotational speed and r is the radial distance of the injecting point from the reactor axis. With respect to the control volume, V_T, the momentum balance gets:

$$\frac{\pi}{4} d_1^2 v_1^2 = \pm \frac{\pi}{4} d_0^2 v_0^2 + \frac{\pi}{4}(d_1^2 - d_0^2) v_e^2$$

where the positive sign applies when the two streams are cocurrent (as in Figure A); the negative sign, when they are countercurrent. Since $d_0 \ll d_1$ and $v_o \leq v_e$, we obtain

$$v_1 \cong v_e$$

so that the total flow rate entering into the jet volume V_T is in first approximation:

$$Q_r \cong \frac{\pi}{4}(d_1^2 - d_0^2) v_e$$

It is important to note that this flow rate is, in a large range of operating conditions, practically independent from the input flow rate.

Manuscript received July 20, 1982; revision received May 11, and June 10, 1983.